CLUSTER ANALYSIS FOR FISSILITY PREDICTION IN VACA MUERTA FORMATION USING LOG DATA

Lucía I. Martín[1], Denis Marchal[2], Claudio Naides[2], Silvia Barredo[1,3]

1: Instituto Tecnológico de Buenos Aires. lucmartin@itba.edu.ar

2: Pampa Energía. denismarchal@pampaenergia.com, claudionaides@pampaenergia.com

3: Universidad de Buenos Aires. sbarredo@fi.uba.ar

Keywords: Vaca Muerta Formation, fissility, cluster analysis

RESUMEN

Cuando una roca de grano fino es expuesta en superficie puede permanecer masiva o partirse a lo largo de planos paralelos a la estratificación si la roca es físil. La fisilidad es una propiedad estructural revelada por la meteorización por la que una roca se rompe aprovechando planos de debilidad. Estos planos de debilidad (o de fisilidad) dependen de numerosos factores tales como la litología, fábrica, procesos diagenéticos y contenido de materia orgánica y pueden influenciar la eficiencia del fracturamiento hidráulico de un play no convencional como la Formación Vaca Muerta. El presente trabajo se focaliza en el análisis de la fisilidad en 4 testigos corona que abarcan más de 300 metros de la Formación Vaca Muerta. El estudio de las mismas resultó en un índice compuesto por 4 clases de diferente grado de fisilidad (DAD, Drying Alcohol Discontinuities). A través de una clasificación supervisada basada en el algoritmo de MRGC (Multi-Resolution Graph-based Clustering) se relacionó esta información con perfiles de pozo e imágenes microresistivas. De esta manera, se consideraron simultáneamente diversos controles en la fisilidad, como la composición (gamma ray y factor fotoeléctrico), las propiedades geomecánicas (perfil sónico) y la textura de la roca (resistividad somera). Los modelos resultantes reprodujeron el índice de DAD con un razonable ajuste en las coronas estudiadas. A fin de caracterizar los intervalos de diferente fisilidad con su respuesta mecánica, se complementó el estudio con análisis geomecánicos. Las rocas de mayor fisilidad corresponden a las muestras de menor resistencia y tenacidad y con mayor anisotropía.

INTRODUCTION

Fissility is defined as the ability of fine-grained rocks to split along finely spaced surfaces parallel to the bedding (Lewis 1924; Ingram 1953; Pettijohn 1975, Bates and Jackson 1987; Sintubin 1994; Potter *et al.* 2005). Although this property is revealed by weathering processes when the rock is exposed at outcrops, it corresponds to a structural property associated to the rock genesis (Lewis 1924; Byers 1974). As fissility impacts on mudstone petrophysical properties such as porosity and permeability (Curtis *et al.* 1980) as well as on their anisotropy (Daigle and Dugan

2011), the fissility degree of a mudstone should influence in the hydraulic stimulation efficiency of an unconventional play as Vaca Muerta Formation.

Recent studies in different basins indicate that mudstone successions are strongly variable both in the lateral and vertical directions, producing a strong impact on hydrocarbon recovery in unconventional plays (Dawson and Almon 2010; Przywara *et al.* 2011; Fairbanks and Ruppel 2012). Several studies demonstrate that Vaca Muerta Formation presents much greater heterogeneity compared to other unconventional shale plays (Cobbold *et al.* 1999; Doyle *et al.* 2005; Fantin *et al.* 2014; Convers *et al.* 2017; Romero-Sarmiento *et al.* 2017; Capelli *et al.* 2018; Comerio *et al.* 2018; Fialips *et al.* 2018; Małachowska *et al.* 2019; Kietzmann *et al.* 2020; Małachowska *et al.* 2022). In spite of the numerous studies addressing the heterogeneity of the Vaca Muerta Formation (Sagasti *et al.* 2014, Stinco and Barredo 2014, Zeller *et al.* 2015; Ortiz *et al.*, 2016 González Tomassini *et al.* 2017, Boitnott *et al.* 2018, Casala *et al.* 2019), scarce information is found about the role of fissility planes in these rocks.

The present study comprises the fissility analysis of 4 cores related to the basal part of the Vaca Muerta Formation and extracted from wells located in the center of the basin. The fissility degree of the cored rocks is related to the log response by means of clustering analysis in order to generate a model to predict this property in subsurface rocks. Geomechanical laboratory studies are also included to estimate the relationship between rheological behavior and fissility degree.

GEOLOGICAL SETTING

The Neuquén Basin is a triangular shaped depocenter developed at the western margin of South America as a series of narrow and isolated half-grabens during the Late Triassic by the extensional collapse of the Late Paleozoic orogen (Vergani *et al.* 1995; Howell *et al.* 2005). During the Early Jurassic, the change from mechanical to thermal subsidence led to the amalgamation of previous isolated topographic lows in broader depocenters constituting a back-arc basin associated with the subduction of the proto-Pacific crust (Uliana *et al.* 1989; Uliana and Legarreta 1993; Legarreta and Gulisano 1989; Vergani *et al.* 1995; Legarreta and Uliana1996b; Howell *et al.* 2005). During this period, the basin was connected to the proto-Pacific Ocean by gaps in the arc (Spalletti *et al.* 2000; Macdonald *et al.* 2003). A complex series of transgressive-regressive cycles developed during this period as a result of subsidence rate variations, eustatic sea-level fluctuations, and localized uplifts (Gulisano *et al.* 1984; Legarreta and Gulisano 1989; Legarreta and Uliana 1991, 1996a, b). In this context was deposited the Vaca Muerta-Quintuco system, being part of the shallowing-upward cycle of the lower Mendoza Group Mesosequence (Legarreta and Gulisano 1989). The Vaca Muerta Formation includes the slope and basinal deposits characterized by fine-grained sediments with high organic matter content related to the foreset and bottomset of the of the prograding clinoforms that form the system (Desjardins *et al.* 2016). Towards the east these rocks grade into shoreface deposits of the Quintuco Formation that constitutes the topsets of the clinoforms, mostly with coarse-grained sediments and low organic matter content. The studied cores were extracted from wells located at the basin center from the units U1, U2 and U5 according to Desjardins *et al.* (2016) (Fig. 1). The cores 1 and 2 encompass units U1 and U2, whereas rocks in core 3B belong to the bottom part of the unit U5 and core 3A includes rocks coming mainly from the upper part of U2 unit, named subunit U2b.

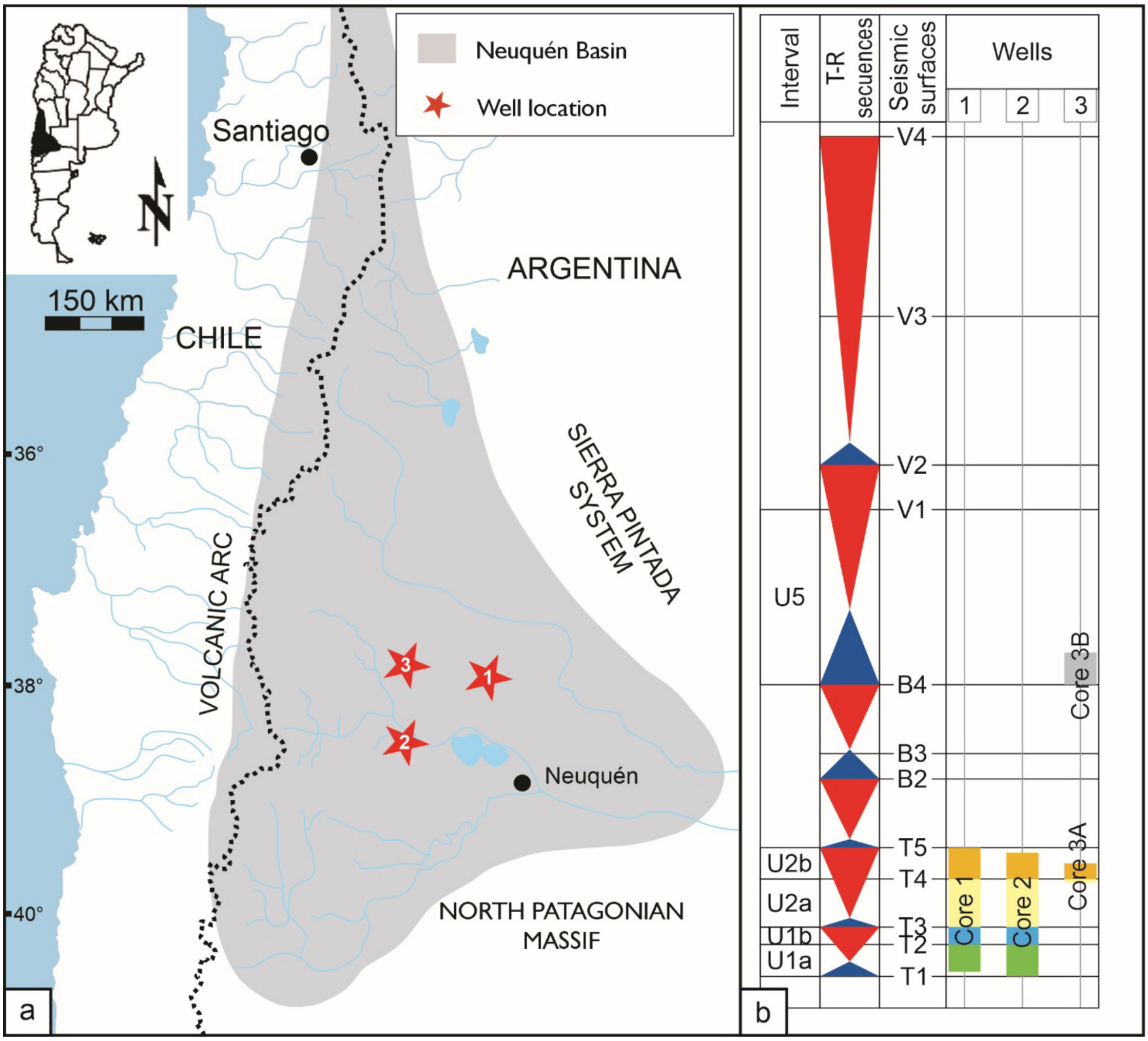

Figure 1. Data set position. a) Location map showing the Neuquén Basin and the cored wells (red stars). b) Stratigraphic intervals cored in each well and the units encompassed according to the nomenclature proposed by Desjardins *et al.* (2016).

METHODOLOGY

Fissility degree was determined by estimating the average spacing of the discontinuities revealed by the differential evaporation of alcohol over a pulled core surface. Depending on the spacing, the rock intervals were classified by the DAD index (Drying Alcohol Discontinuities), where the first class represents the most fissile rock and the fourth the most massive (Fig. 2). For a detailed description of this methodology, the reader is referred to Martin *et al.* (2022, in press).

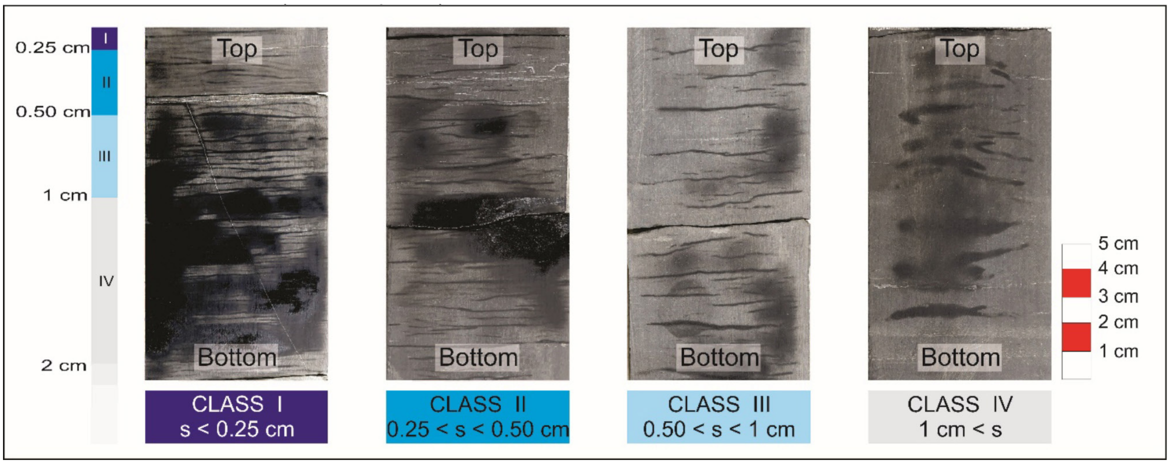

Figure 2. DAD index formed by four classes according to the average spacing between the discontinuities revealed by the differential evaporation of alcohol. Extracted from Martín *et al.* (2022, in press).

The cored rocks encompass more than 300 meters long used to generate predictive models of the DAD index. This tool is used to perform electrofacies modeling, allowing clustering analysis. The process involves the use of clustering algorithms to partition a set of log data into electrofacies units, defined as a “set of log responses that characterizes a sediment and permits the sediment to be distinguished from other” (Serra and Abbott 1982).

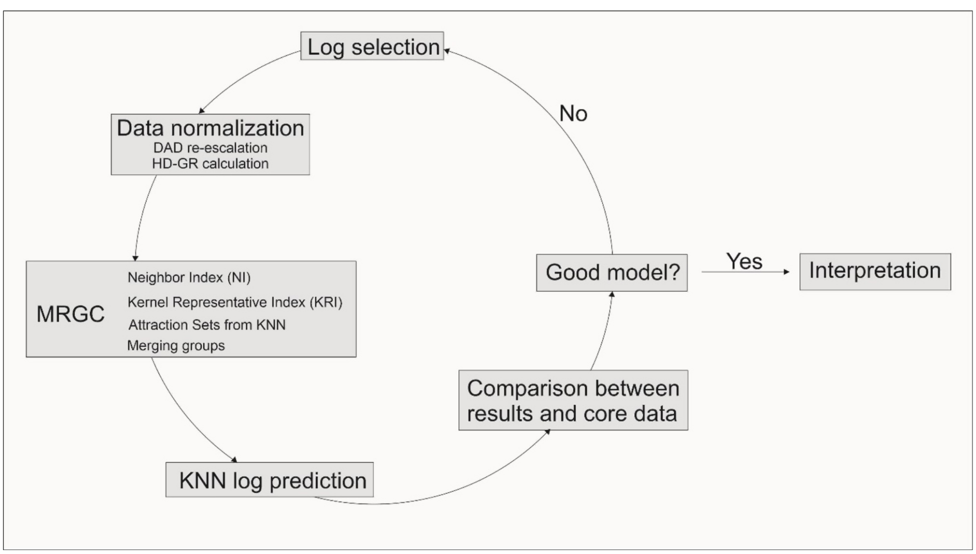

Figure 3. Generalized workflow applied to the DAD index modelling.

The first step in this workflow is the log selection (Fig. 3). Different log combinations were tested to represent the most important features to distinguish between the different DAD classes. In order to eliminate the inconsistency of the actual data dimension of the original log and the fluctuation of the value range, the log data was cleaned and normalized prior to further processing (Dodge *et al.* 2006). The DAD index was also rescaled to the sample rate of the log data to avoid data incompatibility that generates error and bias (Doveton 1994). Subsequently, numerous supervised classifications were performed to reproduce each DAD class from wireline log data applying the Multi Resolution Graph-based algorithm. The information on the calculations involved in this method can be found in Ye and Rabiller (2000). The generated electrofacies were

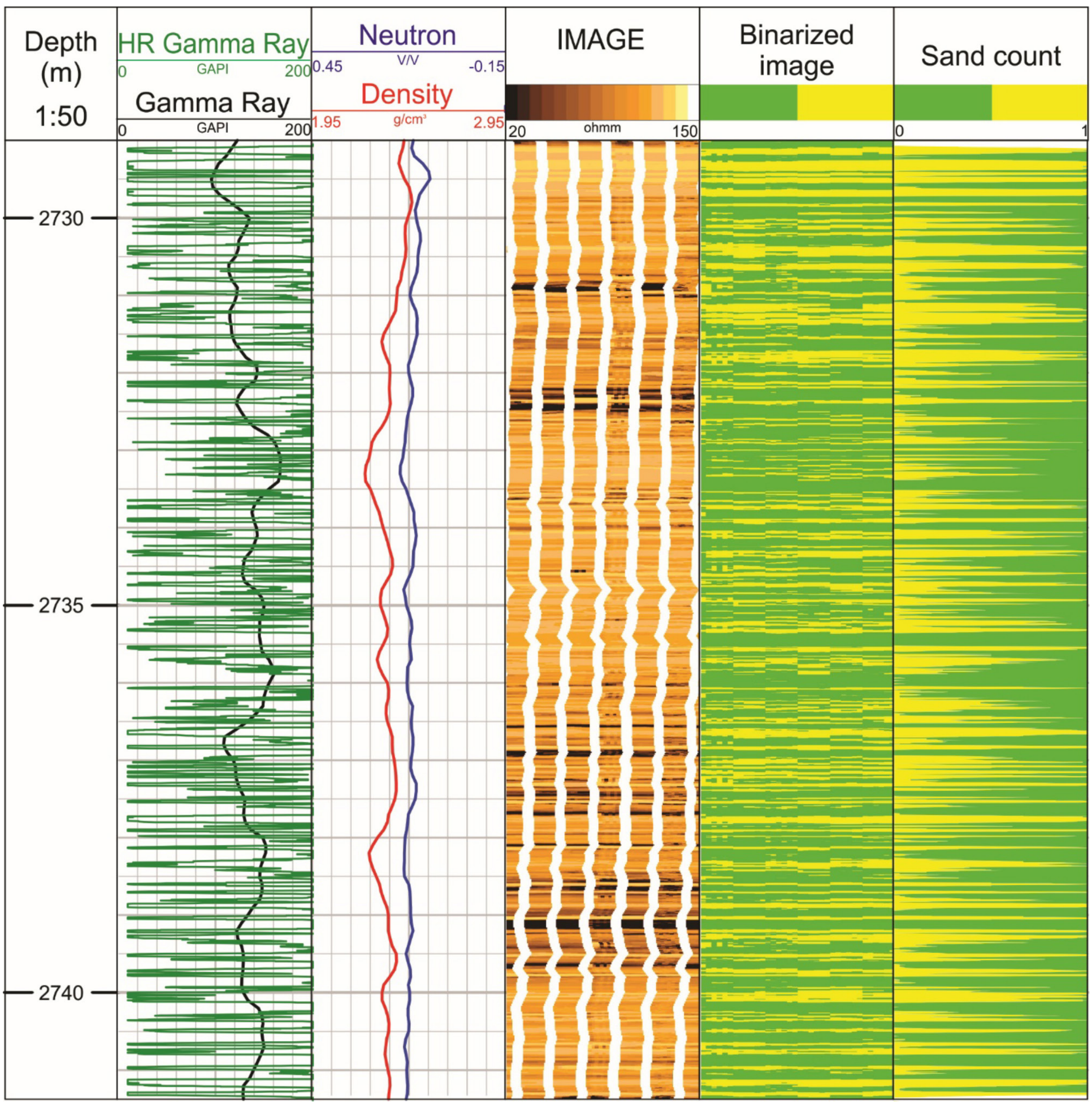

Figure 4. High resolution gamma-ray curve was obtained by binarizing resistivity images and subsequent rescaling of the obtained curve. The cores 1, 3A and 3B were extracted with Water-Based-Mud (WBM) while the core 2 was drilled with Oil-Based-Mud (OBM).

then propagated by means of the K-Nearest Neighbors (KNN) log prediction method, where the Probability Density Functions are estimated in an area from the point to its kth neighbor (Cover and Hart 1967). Comparing the resulting DAD index with the recorded DAD index led us to evaluate the quality of the model. Several iterations were performed until obtaining a good match with the original data, generating the model 1.

To improve the accuracy of the resulting models, a high-resolution gamma ray curve was calculated from the processing of the microresistivity image (Knecht *et al.* 2004, Fig. 4). The equalized image was transformed from a full range of micro-resistivity values into a binary image with two discrete values applying the gamma-ray log as a cutoff. As a result, a curve called ‘Sand Count’ is obtained which was then rescaled using the original gamma-ray range, in order to compute the high-resolution gamma-ray (HR-GR) curve. Finally, the model 2 was built replacing the raw gamma ray log with the HR-GR.

Geomechanical measurements includes uniaxial compressive strength (UCS), multistress compressive testing and elastic parameters, such as Young modulus, Poisson ratio and static and dynamic shear modulus.

RESULTS

DAD clustering analysis

The DAD index shows a variable distribution along the cores with a high frequency alternation between different fissility degree intervals (between 1 and 10 cm, Fig. 5a). In well 1, the fissility is highest at the bottom part of the U1a and U1b subunits and in the middle section of the U2a whereas the U2b presents the lowest fissility degree. The DAD index in the rocks of wells 2 and 3 varies at a high frequency, similar to well 1, but the general tendency of the fissility degree is difficult to establish due to the homogeneous distribution of the different fissility classes and the low presence of DAD class I in the case of core 2 and 3B (Fig. 5b). Nevertheless, similar tendencies of core 2 (well 2) are observed in core 1 (well 1): high fissility degree at the bottom of subunits U1a, U2a and U2b, while the middle part of the U2b corresponds to the less fissile intervals. Lastly, remarkable differences are observed in well 3 between both cored intervals: rocks in core 3B, included in unit U5, are more massive than those of core 3A, corresponding to the subunit U2b.

Model 1 resulted from the combination of four wireline logs: (1) gamma ray and (2) photoelectric absorption factor that represent lithology; (3) shallow resistivity that includes texture information and (4) compressional slowness as a proxy of geomechanical properties. High fissility intervals (DAD classes I and II) are characterized by the lowest resistivity responses, low photoelectric absorption factor measurements, high gamma ray values and a narrow range of compressional

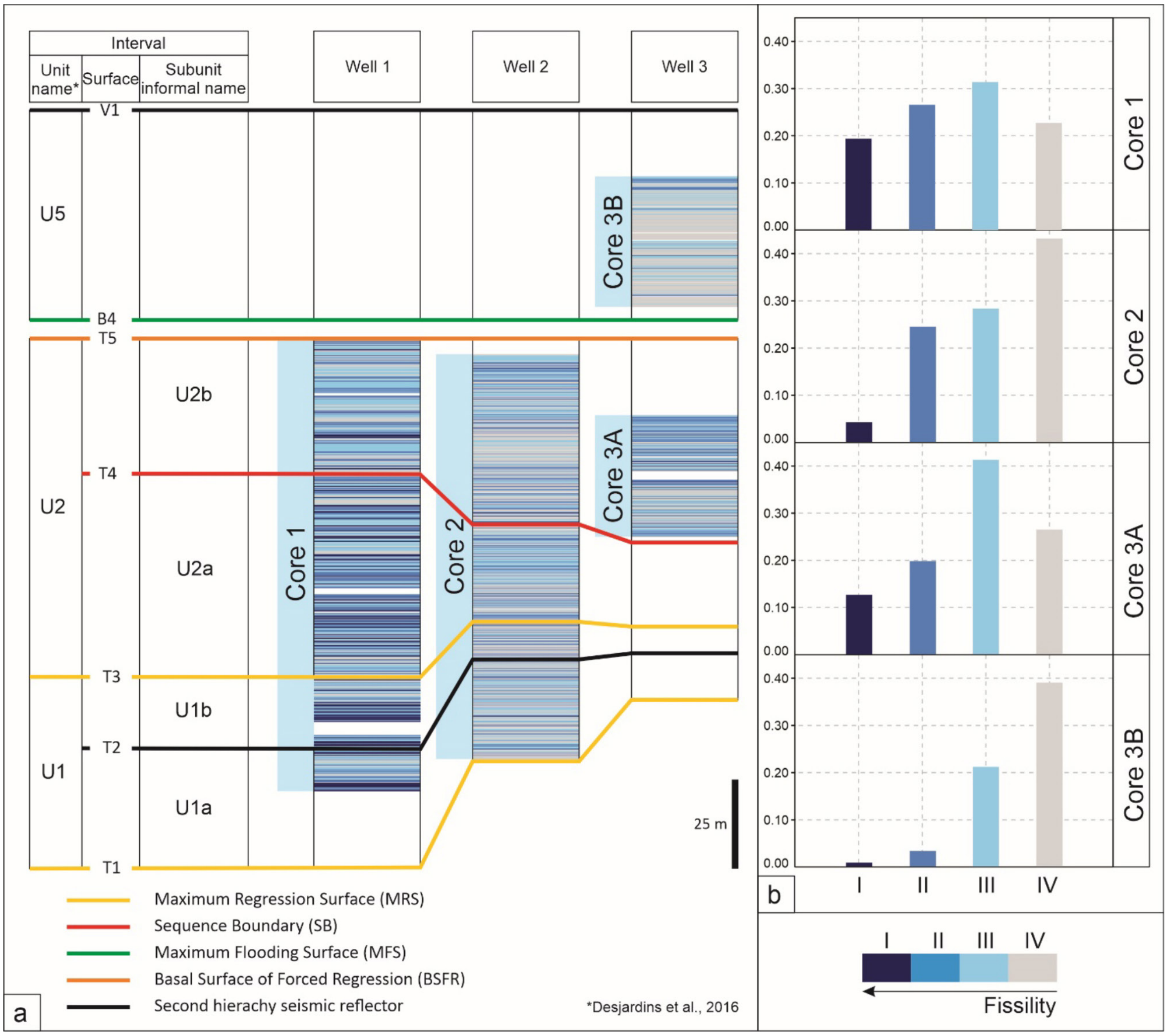

Figure 5. a) DAD index recorded along each core. b) DAD classes frequency distribution per core. Note that core 1 (well 1) and 3A (well 3) display more intervals with high fissility (DAD I and II) than cores 2 (well 2) and 3B (well 3).

slowness. In contrast, DAD classes III and IV intervals with poor or no fissility show low gamma ray responses, a wide range of compressional slowness and high values of photoelectric absorption factor and resistivity.

The synthetic DAD index obtained from model 1 is able to reproduce all the DAD classes with a relatively good adjustment in core 1 with a confidence between 50 and 60 % (Fig. 6b). The adjustment of all DAD classes is higher towards the massive intervals (DAD IV). The model has difficulties in predicting high fissility intervals (excepting core 1). Rocks related to the DAD I are absent in the modeled DAD index of cores 2, 3A and 3B. In the case of core 3B, the model reproduces exclusively DAD classes III and IV.

Model 2, where the gamma ray log was replaced by the HR-GR log (Fig. 6), exhibits a noticeable improvement in the four cores, especially in high fissility intervals. In the case of cores

1 and 3A, the adjustment is almost over 75%. Cores 2 and 3B present a good match (almost over 70% of correspondence) for DAD classes II to IV, whereas the DAD class I is represented with the lowest values of adjustment.

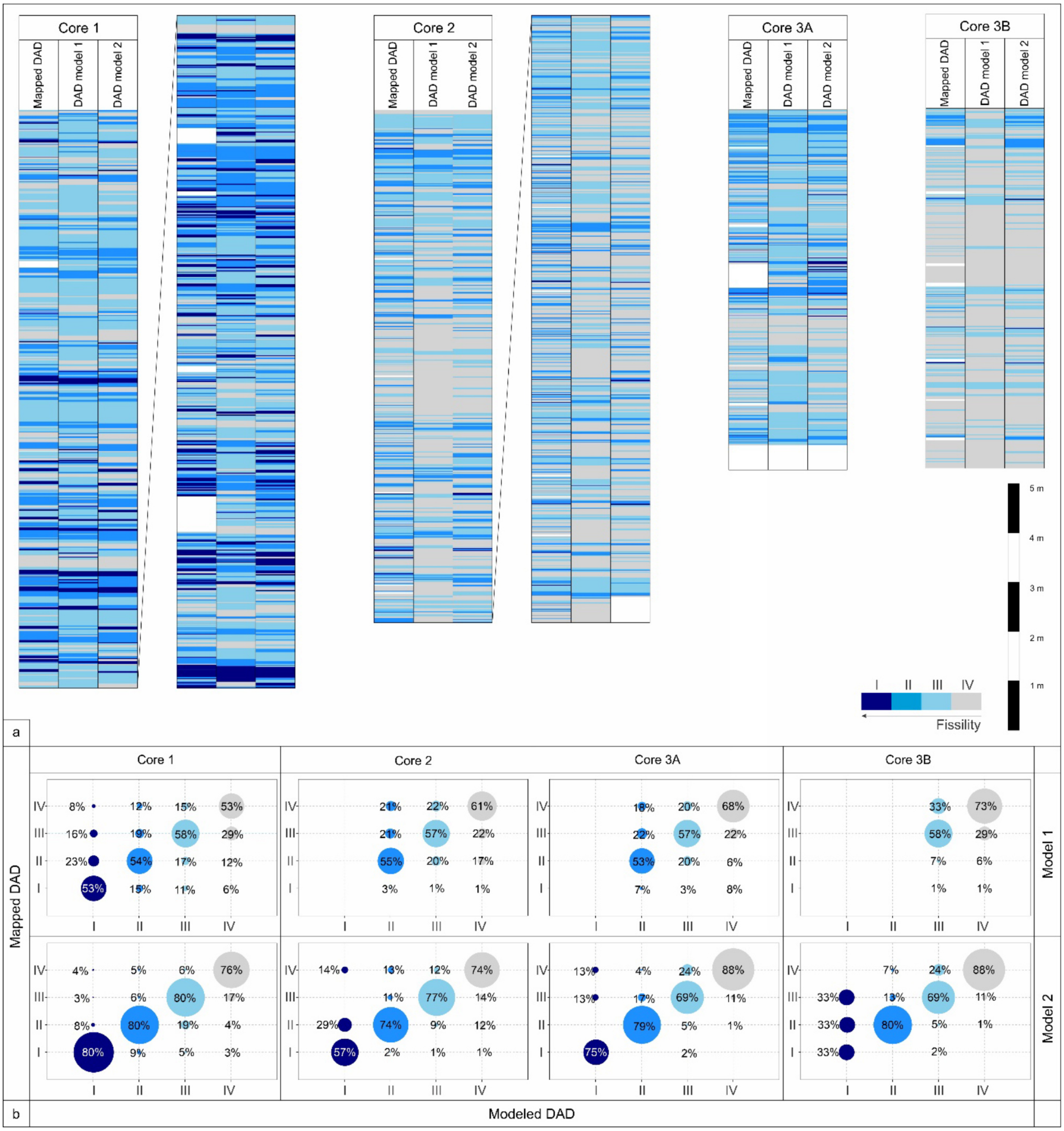

Figure 6. DAD index models. a) Comparison between registered and modeled DAD index. b) The matching degree between recorded and modeled DAD.

Geomechanics and fissility

Geomechanical laboratory tests demonstrate that low fissility and massive intervals are stronger and stiffer than high fissility rocks since their Young modulus, Poisson ratio and Shear modulus are higher (Fig 7a-c). The peak strength measurements performed parallel, perpendicular and at 45 degrees from bedding also show an increase in strength towards low fissility or massive samples, implying that the higher the fissility, the weaker the rock (Fig. 7d). In general, horizontal plugs (parallel to bedding) are stiffer than the vertical ones (perpendicular to the bedding) whereas the oblique plugs (45 degrees to the bedding) are the weakest.

Both static (Fig 7e) and dynamic anisotropy parameters (ε and ε Thomsen 1986, Fig 7f) show that high fissility rocks are significantly more anisotropic than massive samples. Even if most DAD class I rocks were undertested due to the difficulty to sample these highly fissile rocks, the few results obtained for this class confirm the general trends. There are no trends displayed for core 3B since all samples correspond to DAD index equal to IV.

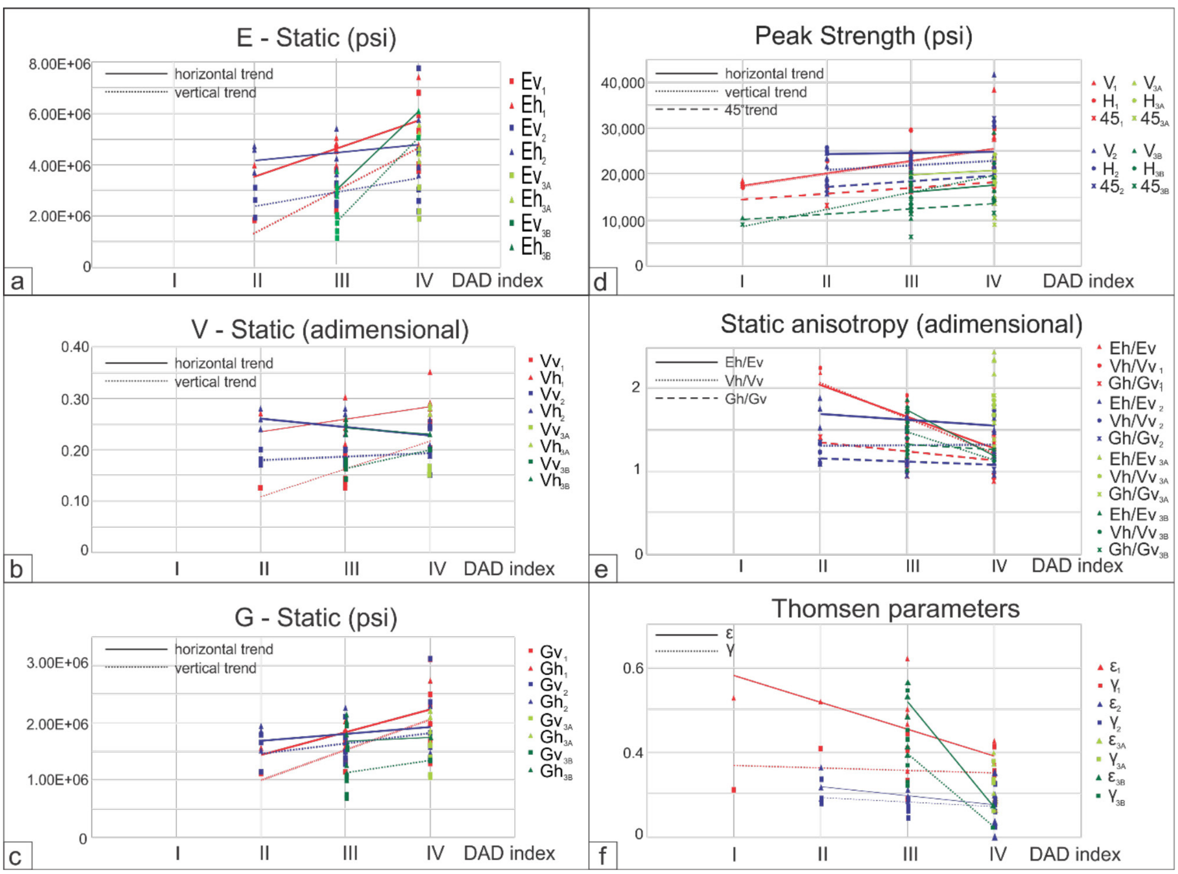

Figure 7. Relationship between geomechanical laboratory tests realized on the core samples and DAD index. a) E, static Young modulus. b) V, static Poisson ratio. c) G, static Shear modulus. d) Peak strength. e) Static anisotropy parameters. f) Anisotropy Thomsen parameters. For E, V, G, vertical (v) and horizontal (h) measurements and trend lines are displayed. For Peak Strength, additional 45° orientation is displayed.

DISCUSSION

DAD clustering analysis

The lack of representation of high fissile rocks by model 1 and the decrease in accuracy of the DAD class I in cores 2 and 3B of model 2 can be related to the minor representation of this type of rocks in the analyzed cores (Fig. 5b). These differences can be related to operational and/or geological factors.

Among the operational factors, there is a considerable difference in the age of the cores. At the time of the study, cores 1 and 3 were 5 years old whereas core 2 was studied only 2 years after its extraction. Fissility is a property that is expressed in outcrops due to decompression and weathering (Ingram 1953; Lundegard and Samuels 1980, Hurst 1987; Potter *et al.* 2005). In a previous study, it has been demonstrated that effective discontinuities in a core evolve through time (Martin *et al.* 2022, in press). It is possible that the newer the core, the less expressed the fissility, which explains the general less representation of high fissility intervals in core 2. Another important difference is that the core 1, 3A and 3B were drilled using Water-Based-Mud (WBM) and the core 2, Oil-Based-Mud (OBM). It could be interpreted that the integrity of cores drilled with WBM decreased due to swelling caused by water in clayey intervals, which accelerated the artificial weathering process of the rock after core acquisition.

From the geological point of view, the rocks included in the core 3B belong to a younger stratigraphic interval (Fig. 5a), located on the foreset of the clinoforms, characterized by a middle to outer ramp/platform sedimentation in suboxic to oxic conditions, where bioturbation was very important (de Barrio *et al.* 2018). The bioturbation homogenizes the sediment and destroys the previous rock fabric, giving rise to a random orientation and a massive rock (Byers 1974; Potter *et al.* 2005). The other cores include lower stratigraphic intervals where sediments were deposited in a more distal environment, mainly corresponding to the bottomsets of the clinoforms. The sediments present lower carbonate content and lesser bioturbation degree (Desjardins *et al.*, 2016; de Barrio *et al.*, 2018). Both parameters inhibit fissility when present (Ingram 1953; Byers 1974; Day-Stirrat *et al.* 2008).

The shallow resistivity log is used in this model as a proxy for rock fabric, since it measures small variations at the first few millimeters of the borehole wall, similar to image logs (Linek *et al.* 2007). This parameter is a key for discrimination between DAD classes (Fig 8), highlighting the relevance of the textural control on fissility. Moreover, in model 2, where the microresistivity image is used to obtain a high-resolution gamma ray curve, the adjustment improves greatly, revealing the importance of input data with a comparable resolution of the studied property. The improvement of the second model relies on the vertical resolution of the HR-GR, comparable to the DAD index variation frequency.

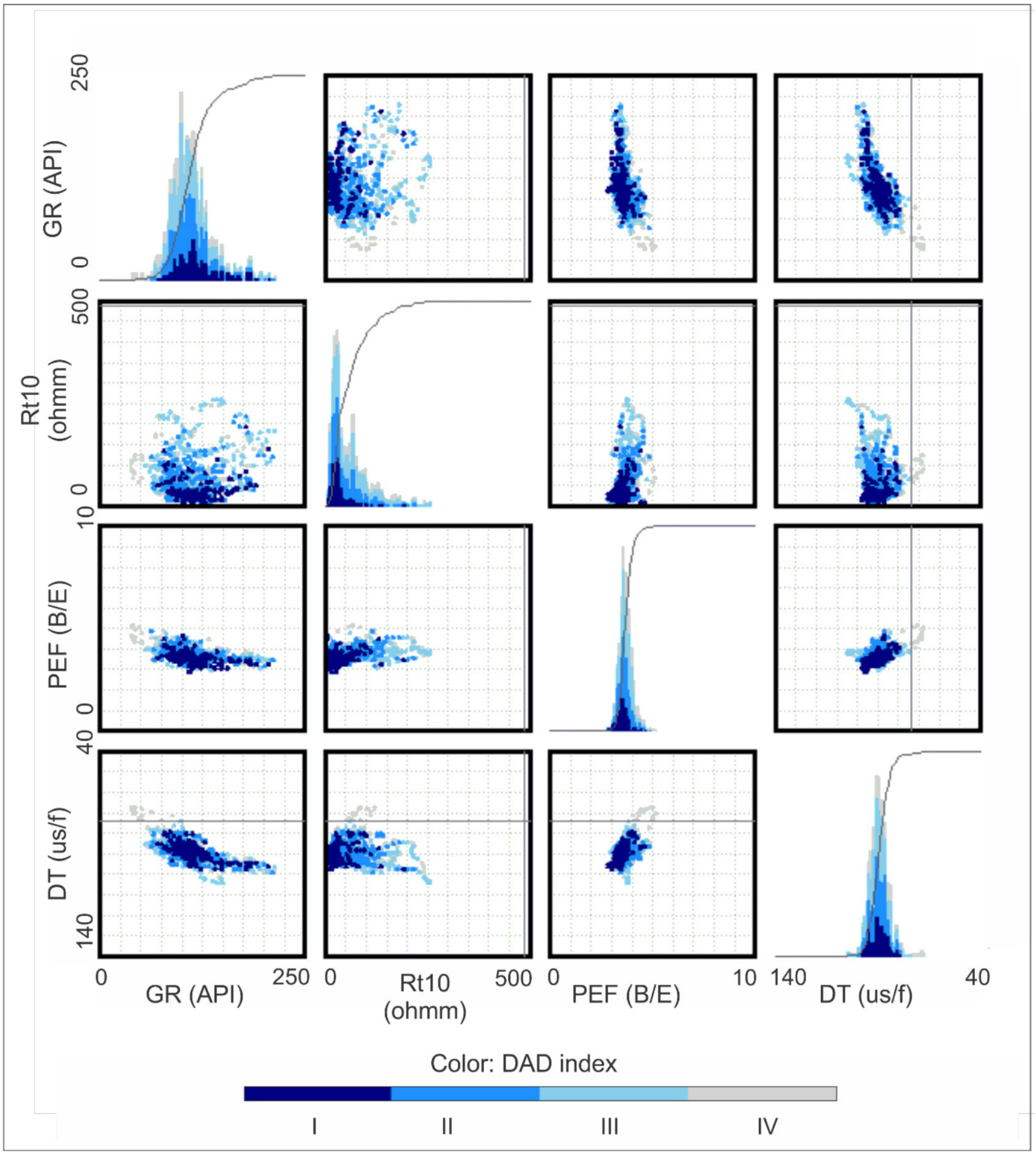

Figure 8. Cross plots of the log responses regarding the DAD index. GR: gamma ray; RT10: shallow resistivity; PEF: photoelectric absorption factor; DT: sonic log. Note that the shallow resistivity (RT10) displays a wider dispersion among the cross plots, implying that it constitutes the best factor to discriminate between the DAD classes.

Geomechanics and fissility

The Vaca Muerta Formation rocks exhibit vertical transverse isotropy (VTI rock type: Thomsen 1986; Ejofodomi *et al.* 2014; Varela *et al.* 2020), where mechanical properties are similar horizontally and vary strongly vertically. Samples characterized by a high fissility index are more anisotropic than their massive counterparts (Fig. 7). Elastic anisotropy of fine-grained rocks is a function of their anisotropic fabric generated by the preferred orientation of platy minerals and the anisotropic elastic properties of the clay minerals (Sone and Zoback 2013; Ejofodomi *et al.* 2014).

Rocks with a high fissility index are weaker (low elastic parameters, Fig. 7a-d) than their massive counterparts due to their components and fabric. The static and dynamic elastic parameters in fine-grained rocks decrease with clay and kerogen content since those are the most compliant constituents (Sone and Zoback 2013).

CONCLUSIONS

- Fissility depends on several factors that have to be considered when building a model to predict their degree by using wireline logs. The most important are the composition (represented by gamma ray and photoelectric absorption factor logs), rock fabric (included in the shallow resistivity log) and their mechanical response to compressional weaves (depicted by the sonic log). Between them, the rock texture resulted in the most important parameter to identify the higher fissile intervals.
- To build a predictive model of any property, the use of data with a vertical resolution similar to the resolution of the modeled characteristic is decisive.
- High fissility intervals present high mechanical anisotropy and are characterized as more compliant than their massive counterparts, thus may affect the efficiency of the hydraulic fracture treatment. The understanding of the generation mechanisms and the indirect prediction of this property can be beneficial for enhancing unconventional hydrocarbon production.

ACKNOWLEDGMENTS

The authors would like to thank Pampa Energía for providing data and permission to present and publish this article. Gratitude is also extended to the Instituto Tecnológico de Buenos Aires (ITBA), TerraTek Schlumberger Reservoir and LCV laboratories for providing the equipment to carry out part of the research.

REFERENCES

Bates, R.L. y Jackson J.A., 1987. Glossary of Geology, 3rd edition. American Geological Institute, 788pp.

Boitnott, G., Louis, L., Hampton, J., Martinez, L., Labeyrie, B., Friry, I. y Lejay, A., 2018. High resolution geomechanical profiling in heterogeneous source rock from the Vaca Muerta Formation, Neuquén Basin, Argentina. 52nd US Rock Mechanics/Geomechanics Symposium, American Rock Mechanics Association, ARMA 18-129, p.8, Washington.

Byers, C.W., 1974, Shale fissility: relation to bioturbation, Sedimentology, 21, 3, p. 479-484, United Kingdom.

Capelli, I.A., Scasso, R.A., Kietzmann, D.A., Cravero, F., Minisini, D. y Catalano, J.P., 2018, Mineralogical and geochemical trends of the Vaca muerta-quintuco system in the Puerta Curaco section, Neuquén basin. Revista Asociación Geológica Argentina. 75, 2, p.210–228, Argentina.

Casala, S., Palacios, J. y Vielma, J., 2019. Fracture Barrier Identification in Unconventional Formation Introducing a New Fracture Barrier Index from Conventional Logs: Vaca Muerta Case. 81st EAGE Conference and Exhibition. Society of Petroleum Engineers, p.3–6. London, UK.

Cobbold, P.R., Diraison, M. y Rossello, E.A., 1999, Bitumen veins and eocene transpression Neuquén basin. Argentina, Tectonophysics 314, 423–442, Netherlands.

Comerio, M., Fernandez, D.E. y Pazos, P.J., 2018, Sedimentological and ichnological characterization of muddy storm related deposits: the upper Hauterivian ramp of the Agrio Formation in the Neuquén Basin, Argentina. Cretaceous Research 85, p.78–94. United States.

Convers, C., Davis, T.L., Hanitzsch, C. y Curia, D., 2017, Rock property prediction for integrated exploration and development. Vaca Muerta Formation, Neuquén Basin, Argentina, First Break 35, p.51–57, Netherlands.

Cover, T. y Hart, P., 1967, Nearest neighbor pattern classification. IEEE transactions on information theory, 13(1), p. 21-27.

Curtis, C.D., Lipshie, S.R., Oertel, G., y Pearson, M.J., 1980, Clay orientation in some Upper Carboniferous mudrocks, its relationship to quartz content and some inferences about fissility, porosity and compactional history, Sedimentology, 27, 3, p.333-339, United Kingdom.

Daigle, H. y Dugan, B., 2011, Permeability anisotropy and fabric development: A mechanistic explanation. Water Resources Research, 47, 12, p.11, United States.

Dawson, W.C. y Almon, W.R., 2010, Eagle Ford shale variability: sedimentologic influences on source and reservoir character in an unconventional resource unit. Gulf Coast Association of Geological Societies, 60, p181-190, United States.

Day-Stirrat, R.J., Aplin, A.C., Srodon, J. y Van der Pluijm, B.A., 2008, Diagenetic reorientation of phyllosilicate minerals in Paleogene mudstones of the Podhale Basin, southern Poland. Clays and Clay Minerals, 56(1), p. 100-111, United States.

De Barrio, A., Ferraresi, P., Köhler, G., Marchal, D., y Blanco, S., 2018, Estudio comparativo de testigos corona de las dos secciones enriquecidas de la Formación Vaca Muerta en la zona de shale gas, noroeste del Engolfamiento Neuquino, Revista de la Asociación Geológica Argentina, 75(2), p. 243-252, Argentina.

Desjardins, P., Fantín, M., González Tomassini, F., Reijenstein, H., Sattler, F., Domínguez, R.F., Kietzmann, D., Leanza, H.A., Bande, A., Benoit, S., Borgnia, M., Vittore, F., Simo, T. y Minisini, D., 2016. Estratigrafía sísmica secuencial. En González, G., Vallejo, M.D., Kietzmann, D., Marchal, D., Desjardins, P., González Tomassini, F., Gómez Rivarola, L. y Domínguez R.F. (eds.) Transecta regional de la Formación Vaca Muerta: Integración de sísmica, registros de pozos, coronas y afloramientos. Instituto Argentino del Petróleo y del Gas, pp.5–22.

Dodge, Y., Cox, D. y Commenges, D., 2006. The Oxford dictionary of statistical terms. Oxford University Press, England, 512pp.

Doyle, P., Poire, D.G., Spaletti, L.A., Pirre, D., Brenchley, P. y Matheos, S.D., 2005, Relative Oxygenation of the Tithonian - Valanginian Vaca Muerta - Chachao Formations of the Mendoza Shelf, Geological Society of London, pp.185–206, United Kingdom.

Doveton, J.H., 1994. Geologic Log Analysis Using Computer Methods. AAPG Computer Applications in Geology, no. 2, 169pp.

Ejofodomi, E.A., Varela, R.A., Cavazzoli, G., Velez, E.I. y Peano, J., 2014. Development of an optimized completion strategy in the Vaca Muerta Shale with an anisotropic geomechanical model, European Unconventional Conference and Exhibition, SPE 167806, p. 25-27. Vienna, Austria.

Fairbanks, M. D., Ruppel, S. C., & Rowe, H. (2016). High-resolution stratigraphy and facies architecture of the Upper Cretaceous (Cenomanian–Turonian) Eagle Ford Group, Central Texas, AAPG Annual Meeting, p.1-3, Long Beach, California.

Fantin, M., Crousse, L., Cuervo, S., Gonzalez, T., Reijenstein, H. y Lipinski, C., 2014. Vaca Muerta stratigraphy in central neuquen basin. Impact on Emergent Unconventional Project, SPE/AAPG/SEG Unconventional Resources Technology Conference (URTeC), p. 1-11, Denver, Colorado, USA.

Fialips, C.I., Labeyrie, B., Burg, V., Maziere, V., Munerel, Y., Haurie, H., Jolivet, I., Lasnel, R., Laurent, J.-P., Lambert, L. y Jacquelin-Vallee, L., 2018. Quantitative mineralogy of Vaca Muerta and alum shales from core chips and drill cuttings by calibrated SEM-EDS mineralogical mapping, Unconventional Resources Technology Conference, pp. 4132-4144, Houston, Texas.

González Tomassini, F., Hryb, D., Palacio, J. P., Lazzari, V., Bertoldi, F., Sagasti, G., 2017. Caracterización e impacto de las heterogeneidades identificadas en subsuelo en la Formación Vaca Muerta, XX Congreso Geológico Argentino, Simposio Geología de la Formación Vaca Muerta, Vol. 67, p.67-71, San Miguel de Tucumán.

Gulisano, C.A., Gutiérrez Pleimling, A.R. y Digregorio, R.E., 1984. Análisis estratigráfico del intervalo Tithoniano – valanginiano (Formaciones Vaca Muerta, Quintuco y Mulichinco) en el suroeste de la provincia de Neuquén, 9° Congreso Geológico Argentino, Actas. vol. 1. p.221–235, Bariloche.

Howell, J.A., Schwarz, E., Spalletti L.A. y Veiga G.D., 2005. The Neuquén Basin: an overview. In The Neuquén Basin, Argentina: A Case Study in Sequence Stratigraphy and Basin Dynamics. En Veiga, G.D., Spalletti, L.A., Howell, J.A. y Schwarz, E. (eds.), Geological Society, Special Publications, 252, p.1-14, London.

Hurst, C.W., 1987. Post-depositional structural changes in clay sediments. Sheffield Hallam University, United Kingdom.

Ingram, R.L., 1953, Fissility of mudrocks. Geological Society of America Bulletin, 64, 8, p. 869-878, United States.

Kietzmann, D.A., González Tomassini, F., y Smith, T. 2020. Grain association, petrography, and lithofacies. En Minisini, D., Fantín, M., Lanusse Noguera, I. y Leanza, H.A. (eds.), Integrated geology of unconventionals: The case of the Vaca Muerta play, Argentina: AAPG Memoir 121, pp. 267–296.

Knecht, L., Ventre, J.B., Leduc, J.P. y Mathis, B., 2004. Improved Formation Evaluation In Thin Beds Using Petrophysical Images, SPWLA 45th Annual Logging Symposium. Noordwijk, Netherlands.

Legarreta, L. y Gulisano, C., 1989. Análisis estratigráfico secuencial de la Cuenca Neuquina (Triásico superior-Terciario inferior). En Chebli, G. y Spalletti, L.A. (eds), Cuencas Sedimentarias Argentinas, Serie Correlación Geológica (Universidad Nacional de Tucumán), pp.: 221–243.

Legarreta, L. y Uliana, M.A., 1991. Jurassic-Cretaceous marine oscillations and geometry of backarc basin fill, Central argentine Andes. En Macdonald, D.I. (ed.), Sedimentation, Tectonics and Eustasy. Sea Level Changes at Active Plate Margins, vol. 12. International Association of Sedimentologists Special Publication, Oxford, pp. 429–450.

Legarreta, L. y Uliana, M.A., 1996a, La sucesión jurásica en el centro oeste de Argentina. Arreglo estratigráfico, secuencias y evolución paleogeográfica. Boletín de Informaciones Petroleras XII (45), p. 66–78, Buenos Aires.

Legarreta, L. y Uliana, M.A., 1996b. The Jurassic succession in west-central Argentina: stratal patterns, sequences and palaeogeographic evolution. Palaeogeography, Palaeoclimatology, Palaeoecology, 1996, vol. 120, no 3-4, p. 303-330, Netherlands.

Lewis, J.V., 1924, Fissility of Shale and Its Relations to Petroleum. Bulletin of the Geological Society of America, 35(3), p. 557-590, United States.

Linek, M., Jungmann, M., Berlage, T., Pechnig y R., Clauser, C., 2007, Rock classification based on resistivity patterns in electrical borehole wall images, Journal of Geophysics and Engineering 4(2), p. 171-183, United Kingdom.

Lundegard, P.D., y Samuels, N.D., 1980, Field classification of fine-grained sedimentary rocks. Journal of Sedimentary Research, 50(3), p. 781-786, United States.

Macdonald, D., Gómez Pérez, I., Franzese, J., Spalletti, L., Lawver, L., Gahagan, L., Dalziel, I., Thomas, C., Trewin, N., Hole, M. y Paton, D., 2003, Mesozoic break-up of SW Gondwana: implications for regional hydrocarbon potential of the southern South Atlantic. Marine and Petroleum Geology, 20(3-4), p. 287-308, Netherlands.

Małachowska, A., Mastalerz, M., Hampton, L., Hupka, J. y Drobniak, A., 2019. Origin of bitumen fractions in the Jurassic-early Cretaceous Vaca Muerta Formation in Argentina: insights from organic petrography and geochemical techniques, International Journal of Coal Geology, 205, p. 155–165, Netherlands.

Małachowska, A., Lis, G. P., Mastalerz, M., Goodarzi, F. y Sanei, H., 2022, The effect of paleo-environment on hydrocarbon generation potential: Example from Vaca Muerta Formation, Neuquén Basin, Argentina. Journal of Petroleum Science and Engineering, 208, 109342, p. 1-14, Netherlands.

Martín, L., Marchal, D., Barredo, S., Naides, C. y Blanco S., 2022, Relationship between fissility, composition, rock fabric and reservoir properties in Vaca Muerta Formation (Neuquén Basin, Argentina): from outcrop to subsurface core data, Andean Geology, en prensa.

Ortiz, A.C., Hryb, D.E., Martínez, J.R. y Varela, R.A., 2016. Hydraulic fracture height estimation in an unconventional vertical well in the Vaca Muerta formation, Neuquén basin, Argentina, SPE Hydraulic Fracturing Technology Conference, Society of Petroleum Engineers, SPE-179145-MS. Texas, USA.

Pettijohn, F.J., 1975. Sedimentary rocks (Vol. 3). Harper & Row, 628 pp.

Potter, P.E., Maynard, J.B. y Depetris, P.J., 2005. Mud and mudstones: Introduction and overview. Springer Science & Business Media. 297pp.

Przywara, M., Howard, A., Hernandez, R. y Brooks, D., 2011, Unconventional reservoir evaluation: focus on the Eagle Ford. Gulf Coast Association of Geological Societies, 61, p. 625-629, United States.

Romero-Sarmiento, M.-F., Ramiro-Ramirez, S., Berthe, G., Fleury, M. y Littke, R., 2017, Geochemical and petrophysical source rock characterization of the Vaca Muerta Formation, Argentina: implications for unconventional petroleum resource estimations. International Journal of Coal Geology, 184, p. 27–41, Netherlands.

Sagasti, G., Foster, M., Hryb, D., Ortiz, A. y Lazzari, V., 2014. Understanding geological heterogeneity to customize field development: An example from the Vaca Muerta unconventional play, Argentina, Unconventional Resources Technology Conference (URTeC), Society of Exploration Geophysicists, American Association of Petroleum Geologists, Society of Petroleum Engineers, p.797-816, Denver, Colorado.

Serra, O. y Abbott, H.T., 1982, The Contribution of Logging Data to Sedimentology and Stratigraphy. Society of Petroleum Engineers Journal, 22(01), p.117–131.

Sintubin, M. 1994, Clay fabrics in relation to the burial history of shales, Sedimentology, 41, 6, p.1161-1169, United Kingdom.

Sone, H. y Zoback, M.D., 2013, Mechanical properties of shale-gas reservoir rocks—Part 1: Static and dynamic elastic properties and anisotropy. Geophysics 78 (5), p. D381-D392, United States.

Spalletti, L.A., Franzese, J., Matheos, S.D. y Schwarz, E., 2000, Sequence stratigraphy in tidally-dominated carbonate-siliciclastic ramp, the Tithonian of the southern Neuquén Basin, Argentina. Journal of the Geologial Society, 157, p. 433–446, United Kingdom.

Stinco, L.P. y Barredo, S.P., 2014. Vaca Muerta Formation: An example of shale heterogeneities controlling hydrocarbon accumulations, Unconventional Resources Technology Conference (URTec), Society of Exploration Geophysicists, American Association of Petroleum Geologists, Society of Petroleum Engineers: p.2854-2868. Denver, Colorado.

Thomsen, L., 1986, Weak elastic anisotropy, Geophysics 51 (1), p. 1954-1966, United States.

Uliana, M., Biddle, K.T. y Cerdan, J., 1989. Mesozoic extension and the formation of Argentine sedimentary basins. En: Tankard, A.J. y Balkwill, H.R. (eds.), Extensional Tectonics and Stratigraphy of the North Atlantic Margins, AAPG Memoir, vol. 46. pp. 599-614.

Uliana, M.A. y Legarreta, L., 1993. Hydrocarbons habitat in a Triassic-to-Cretaceous sub-Andean setting: Neuquen Basin, Argentina. J. Pet. Geol. 16, 397-420.

Varela, R.A., Marchal, D, Cuervo, S, Lombardo, E.F., Perl, Y.P., Hryb, D.E., Pateti, P. y Nielsen, O. 2020. Geomechanics: Pressure, stress field, and hydraulic fractures. En Minisini, D., Fantín, M., Lanusse Noguera, I. y Leanza, H.A. (eds), Integrated geology of unconventionals: The case of the Vaca Muerta play, Argentina, The American Association of Petroleum Geologists (AAPG) Memoir 121, pp. 351–376.

Vergani, G.D., Tankard, A.J., Belotti, H.J. y Welkink, H.J. 1995. Tectonic evolution and paleogeography of the Neuquén Basin, Argentina. En Tankard, A.J.; Suarez Soruco, R.; Welsink, H.J. (eds), Petroleum Basins of South America, The American Association of Petroleum Geologists (AAPG), Memoir 62, pp. 383–402.

Ye, S. y Rabiller, P., 2000. A New Tool for Electro-

Facies Analysis: Multi-Resolution Graph-Based Clustering, SPWLA 41st Annual Logging Symposium, p.1–14, Dallas, Texas.

Zeller, M., Reid, S.B., Eberli, G.P., Weger, R.J. y Massaferro, J.L., 2015, Sequence architecture and heterogeneities of a field–Scale Vaca Muerta analog (Neuquén Basin, Argentina)–From outcrop to synthetic seismic, Marine and Petroleum Geology, 66, p.829-847, Netherlands.